THE AUTOGYRO FOR SHIP PROPULSION

by

N. Bose*

Summary

A strip theory approach is described which is designed to obtain the lift and drag coefficients of a wind turbine rotor operating as an autogyro. This theory is an extension of the autogyro theory which was developed during the 1920's and 1930's. The theory has been extended to include the effects of varying blade planform, blade section and blade twist. This was necessary in order to evaluate the performance of the variable pitch rotors used for the propulsion of marine craft when operating in beam winds in the autogyro mode. Rotors with flapping blades were not considered. A computer program has been written incorporating this method.

Results have been obtained for two example autogyro rotors using this program and these are presented here to give an idea of the typical performance of a wind turbine rotor when operating in the autogyro mode. The characteristics of autogyros are discussed in relation to their use as propulsion systems for wind propelled marine vehicles.

1. Introduction

The use of wind turbines as a means of harnessing the energy available in the wind for the propulsion of marine vehicles has been described by a number of researchers including the author [1, 2, 3, 4]. The extraction of power from the wind, when a turbine operates as a windmill, can be predicted using a version of the vortex theory of the airscrew and this has been well documented by Glauert [5] and more recently by workers concerned with the design of aerogenerators. To drive a ship directly into the wind, the turbine must operate as a windmill and the propulsive force is obtained from a water screw which is driven by the turbine. On courses across the wind, a larger propulsive force is obtained if the turbine is operated as a freely rotating autogyro and the propulsion is achieved in a similar manner to a sail driven vessel. This principle was used by two experimenters, one in America and one in Britain, in the 1930's, who both fitted a two-bladed horizontal axis autogyro rotor to a mast on a small yacht in place of the conventional sails [6, 7]. The way in which an autogyro rotor can replace an aerofoil was first exploited by De La Cierva, who used these rotors in place of the wings of aircraft [8, 9, 10, 11]. Unfortunately, the lift-drag ratio is less for the autogyro than for the aerofoils which form the wings of an aeroplane [12] and as a result, autogyros were not universally adopted on aircraft. This is not the case when comparing autogyros with other wind propulsion devices and the advantage of the use of wind turbines for propulsion make it necessary to be able to predict their performance in this mode of operation also.

The method which is described here for the calculation of the forces incident on a wind turbine rotor when in operation as an autogyro, is designed to give approximate results to this complex problem in as simple a manner as possible. This approach was considered to be justified in establishing the overall performance of the autogyro rotor as a propulsive device on a moving vehicle and, in particular, for comparing a variety of rotors with differing geometries. The calculations were, therefore, made on a fixed rotor (i.e. a rotor without flapping blades) but in contrast to the theories presented by Glauert [5, 13], Lock [14] and Wheatley [15] for fixed rotors, allowances were made for varying blade planform, section and twist.

*) Research Fellow, Department of Naval Architecture and Ocean Engineering, University of Glasgow, U.K.

2. Theoretical background

An autogyro at an angle of incidence to the incoming flow of i can be considered to be a windmill descending with an axial velocity $V\sin i$ and with a velocity of sideslip $V\cos i$. Owing to the fact that the velocity of sideslip is considerably greater than the axial velocity, it is assumed that the induced velocity arising from the system of trailing vortices will correspond more closely to that of an aerofoil than to that usually associated with a windmill. It is also assumed that this induced velocity has a constant value over the whole rotor disc. The resultant velocity V' experienced by the autogyro is the resultant of the apparent wind velocity V and the axial induced velocity v, and is given by

$$V'^2 = (V\sin i - v)^2 + V^2\cos^2 i$$

Taking the axial induced velocity to be

$$v = \frac{T}{2\pi R^2 \rho V'}$$

from the equation for the induced velocity of the monoplane aerofoil where T is the thrust force and R

the radius of the rotor, and writing the axial velocity through the disc as

$$u = V\sin i - v = \Omega Rx$$

the equation for the induced velocity can then be expressed in the form

$$\lambda \sin i = x + \frac{\frac{1}{2}T_c}{\sqrt{\lambda^2 \cos^2 i + x^2}} \qquad (1)$$

where λ is the inverse of the tip speed ratio normally associated with a windmill

$$\lambda = \frac{V}{\Omega R}$$

and T_c is the thrust coefficient given by

$$T = T_c \pi R^2 \rho \Omega^2 R^2$$

Similarly, the remaining force and moment coefficients are non-dimensionalised as follows

Longitudinal force	H	=	$H_c \pi R^2 \rho \Omega^2 R^2$
Side force	Y	=	$Y_c \pi R^2 \rho \Omega^2 R^2$
Torque	Q	=	$Q_c \pi R^2 \rho \Omega^2 R^3$
Rolling moment	L	=	$L_c \pi R^2 \rho \Omega^2 R^3$

Considering the flow at a blade element and referring to Figure 1, the velocities U_x and U_y are

$$U_x = U\cos\phi = r\Omega + V\cos i \sin\psi$$

$$U_y = U\sin\phi = xR\Omega - r\dot{\beta} - V\beta\cos i \cos\psi$$

and the velocity along the blade $= \mu R\Omega \cos\psi$

where $V\cos i = \mu R\Omega$, and U and ϕ are defined for the blade element in Figure 2. β is the sum of the angular displacement of the blade and the coning angle of the blade (β_o) and $\dot{\beta}$ is the velocity of flapping. The angular displacement and the velocity of flapping are both zero in this case for fixed blades. Also for small ϕ it is possible to write $U_x = U$ and $U_y = \phi U$.

2.1. *Thrust force*

To obtain the overall thrust force on the rotor, the thrust force on a blade element is first considered. The

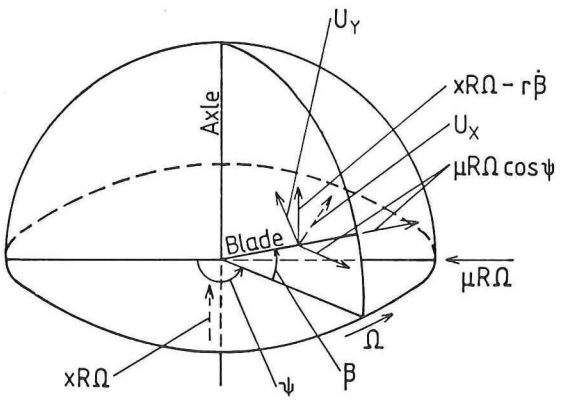

Figure 1. Velocities on a blade of the autogyro.

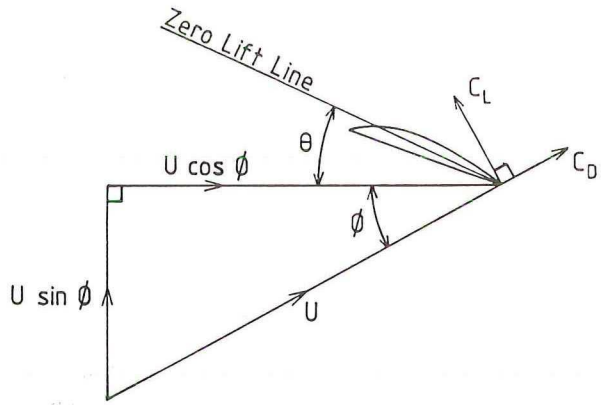

Figure 2. Flow at a blade element.

coefficient of the force parallel to the axis of the rotor is equal to $C_L \cos\phi + C_D \sin\phi$, which for small C_D and ϕ can be taken to be approximately C_L. On one blade

$$\frac{dT_1}{dr} = \frac{1}{2}\rho c U^2 a(\theta + \phi)$$

where a is the lift curve slope, c is the chord length and $(\theta + \phi)$ is the angle of incidence α_i (Figure 2). In these calculations, the lift curve slope has been taken to be linear and equal to 2π,

$$C_L = 2\pi\alpha_i$$

and the drag coefficient has been taken to be constant ($C_D = \delta$). By substituting for the velocity components and summing over all the blades of the rotor, the total thrust coefficient on an element becomes

$$\frac{dT_c}{dr} = \frac{Bca}{2\pi R^2}\left[\frac{\theta r^2}{R^2} + \frac{xr}{R} + \frac{\theta\lambda^2\cos^2 i}{2}\right]$$

where B is the number of blades and r is the radius of the element.

It should be noted that when summing over the number of blades of the rotor the periodic terms in ψ which arise from the velocity terms, either disappear (cos, sin, cos sin, $\cos^3$, $\sin^3$, $\sin^2\cos$, $\cos^2\sin$ terms) or become equal to $B/2$ times the coefficient ($\sin^2$, $\cos^2$ terms). This is true for rotors with three or more blades, but for two bladed rotors, while the averaged result is given over the cycle by adopting this procedure, the force values will in fact oscillate over the cycle. The amplitude of this osciallation depends on which terms of the force coefficient are involved with the oscillatory terms of ψ.

To illustrate this point it can be seen by expanding the thrust force on one blade that

$$\frac{dT_1}{dr} = \frac{1}{2}\rho c a U^2(\theta + \phi)$$

$$= \frac{1}{2}\rho c a(\theta U^2 + U^2\phi)$$

$$= r^2\Omega^2\theta + xrR\Omega^2 + \theta V^2\cos^2 i \sin^2\psi$$

$$+\sin\psi\ \{\theta\, 2r\Omega V\cos i + xR\Omega V\cos i\}$$
$$-\cos\psi\ \{\beta_o r\Omega V\cos i\}$$
$$-\cos\psi\sin\psi\ \{\beta_o V^2\cos^2 i\}$$

Summing over the whole rotor (i.e. for all blades) gives

$$\frac{dT}{dr} = \tfrac{1}{2}\rho ca\,B\left\{r^2\Omega^2\theta + xrR\Omega^2 + \frac{V^2\theta\cos^2 i}{2}\right\}$$

where the periodic terms have disappeared or been replaced by $B/2$ depending on the power of the sin and/or cos terms.

2.2. *Torque*

The coefficient of force tangential to the blade is $-(C_L\sin\phi - C_D\cos\phi)$ which can be approximated to $-(C_L\phi - C_D)$ for small ϕ (positive when it opposes the motion of the rotor). This gives the torque on an element of one blade of the autogyro as

$$\frac{dQ_1}{dr} = \tfrac{1}{2}\rho cr(\delta U_x^2 - a\theta U_x U_y - aU_y^2)$$

where δ is the drag coefficient and equal to twice the value used in References [5, 13, 14 and 15]. This gives the total torque coefficient on an element summed over all the blades as

$$\frac{dQ_c}{dr} = \frac{Bcr}{2\pi R^3}\left[\frac{\delta r^2}{R^2} - \frac{a\theta xr}{R} - ax^2 + \tfrac{1}{2}\delta\lambda^2\cos^2 i - \tfrac{1}{2}a\beta_o^2\lambda^2\cos^2 i\right]$$

Now at each blade element B, c, r, R, δ, a, θ and β_o are known. Hence for a range of $\lambda\cos i$ (which is constant for the autogyro at each state of operation) it is possible to get dQ_c/dr in terms of x for each element and integrate these values numerically to get the torque coefficient Q_c for the whole rotor in terms of x. Since the torque coefficient for the whole rotor is zero we have a quadratic in x which can be solved for the roots. In the computer program, 10 stations were taken along the blades of the rotor from $0.1R$ to $1.0R$ in steps of $0.1R$, the details of the blade being provided at each station.

2.3. *Longitudinal force*

The longitudinal force for a blade element, which is taken to be positive for a downwind force, is given for one blade by

$$\frac{dH_1}{dr} = \frac{1}{r}\frac{dQ_1}{dr}\sin\psi - \beta_o\frac{dT_1}{dr}\cos\psi$$

where ψ is the rotated angle of the blade from the downwind position. The downwind force coefficient for a blade element summed over all the blades becomes

$$\frac{dH_c}{dr} = \frac{Bc}{2\pi R^2}\lambda\cos i\left[\frac{\delta r}{R} - \frac{a\theta x}{2} + \frac{a\beta_o^2 r}{2R}\right]$$

2.4. *Sideways force*

The sideways force for a blade element, which is taken to be positive to port for an autogyro rotating in an anti-clockwise direction when viewed from above, for one blade, is given by

$$\frac{dY_1}{dr} = \frac{dQ_1}{rdr}\cos\psi + \beta_o\frac{dT_1}{dr}\sin\psi$$

When summed over all the blades and non-dimensionalised this becomes

$$\frac{dY_c}{dr} = \frac{3}{4}\frac{Bca}{\pi R^2}\beta_o\lambda\cos i\left[\frac{\theta r}{R} + x\right]$$

2.5. *Rolling moment*

The rolling moment for the same autogyro rotor with fixed blades, for the blade element is

$$\frac{dL_1}{dr} = r\sin\psi\frac{dT_1}{dr}$$

positive rolling moment to port for the anti-clockwise rotation described as for the sideways force. Non-dimensionalising and summing over all the blades gives

$$\frac{dL_c}{dr} = \frac{Bca\lambda\cos i}{4\pi R^2}\left[\frac{2\theta r^2}{R^2} + \frac{xr}{R}\right]$$

For a rotor with flapping blades this rolling moment disappears.

3. The calculation procedure

The calculation starts by obtaining the value of x from the torque equation, as described previously under the section on the torque coefficient, for a range of values of $\lambda\cos i$. In general two values for x are found, but over the range of validity of the theory, one of these is normally negative, indicating a reversed flow. The positive value is therefore the only real solution.

Once the value of x has been identified, the remaining force and moment coefficients can be calculated. Again these are calculated at different blade elements and integrated numerically over the radius to obtain the overall force coefficient.

It is then possible to obtain the value of the angle of incidence, i, from equation (1), as well as the value of the speed ratio term λ for each value of $\lambda\cos i$. It is then an easy matter to obtain the lift and drag coefficients from the following equations

$$C_L = \frac{2}{\lambda^2}(T_c\cos i - H_c\sin i)$$

$$C_D = \frac{2}{\lambda^2}(T_c \sin i + H_c \cos i)$$

and the overall force coefficient C_{TA} and aerodynamic drag angle ϵ_A are found as follows

$$C_{TA} = \sqrt{C_L^2 + C_D^2}$$

$$\epsilon_A = \tan^{-1}\left(\frac{C_D}{C_L}\right)$$

The numerical integrations over the radius are made using Simpson's rule.

The theory breaks down for large angles of incidence , i, above about 45 degrees where the rotor's action becomes more like that of a true windmill, when the angle of incidence of the inflow to the blades exceeds the angle required for stalled flow to occur on the blades and also if ϕ is not small. At each point of operation for which the calculation is carried out, the maximum angle of attack for each blade element considered is calculated. This is done by calculating the inflow angle ϕ every five degrees as the blade rotates about the rotor axis from the equation

$$\phi = \tan^{-1}\left(\frac{x - \lambda\beta_o \cos i \cos\psi}{r/R + \lambda \cos i \sin\psi}\right)$$

and finding the maximum value. The maximum angle of attack is equal to $(\phi + \theta)$ where θ is the blade angle. If r/R is less than $\lambda \cos i$ a reversed flow will occur on the blade element over a part of the cycle. This normally occurs at low tip speed ratios, over the inner portion of the blade, on the blade which is travelling in the same direction as the apparent wind. The situation at the blade element, whether reversed flow occurs, the section is stalled or unstalled, together with the maximum angle of attack, is displayed on the computer printout. It must be remembered that this is the worst condition over the full cycle of the blade and over most of the cycle, lift will be produced in the normal manner. Furthermore, this adverse flow normally occurs over the inner portions of the blades whose contribution to the total force coefficients is small in comparison to the outer portion of the blades. A certain amount of reverse flow and stall may be tolerated in these regions before any appreciable errors in the theoretical force coefficients are produced.

4. Theoretical predictions for two autogyro rotors

The program was first run for the autogyro example given in Reference [5] (Autogyro A). This is an autogyro rotor with a constant chord length, a solidity of 0.2, a drag coefficient of 0.012, and a blade angle of 2 degrees. The results are shown in Figure 3. There are no substantial differences in the drag results, but

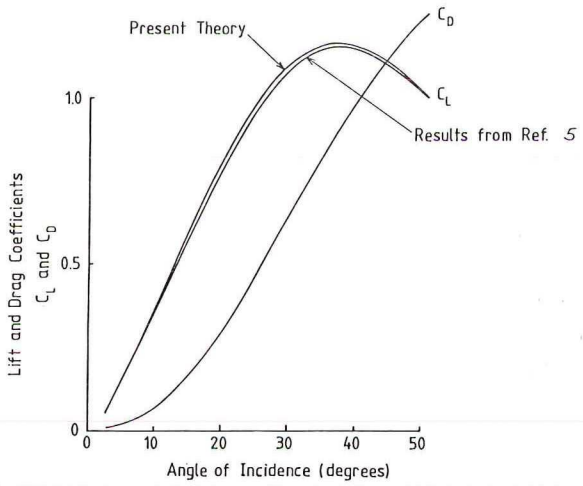

Figure 3. Comparison between the present theory and Glauert's calculations for autogyro A at a blade rotation of $-2°$.

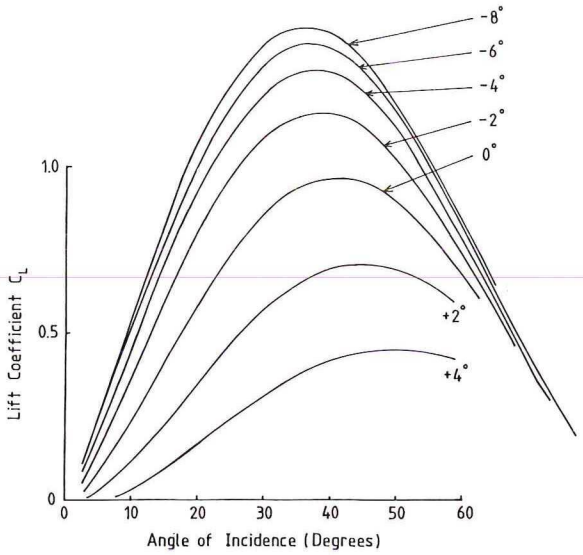

Figure 4. Lift coefficients for autogyro A. Numbers denote blade rotations.

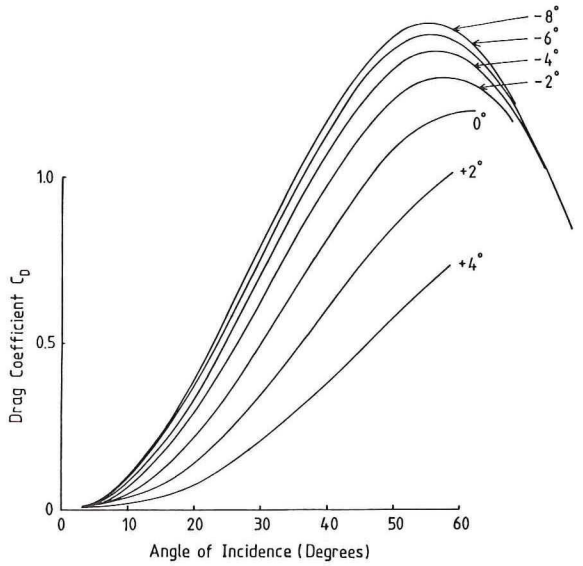

Figure 5. Drag coefficients for autogyro A. Numbers denote blade rotations.

the lift coefficients are very slightly higher because of the difference in the lift curve slope. Glauert takes the lift curve slope to be 6, whereas in this work a value of 2π was used.

Figures 4 and 5 show what happens to the lift and drag values as the pitch of this rotor is altered. The rotations were from +4° to −8° about the design pitch value of 0°. A design pitch value of 0° means that the blades are untwisted. A positive rotation is in a direction towards the fully feathering position (Figure 2). For this rotor a blade rotation of 0° meant that the blades were unpitched; that is, flat in the plane of rotation of the autogyro, and it can be seen that a useful degree of lift is obtained at this setting. Both the lift and the drag increase as the angle of attack of the blades is increased, although this increase becomes smaller as the blades near their angle of stall. Between a blade rotation of −8 and −10 degrees stall occurs on the blades and the theory ceases to be valid. Stall occurred fairly evenly over the span of the blades with this rotor.

Figures 6 and 7 show similar curves for the three bladed wind turbine which is shown in Figure 12 (Autogyro B). This turbine has a design pitch of 2 metres and hence a large degree of twist in the blades along the span. The blades are tapered from a chord of 0.3 m at the root to 0.15 m at the tip, and the blade section incorporates camber with a design lift coefficient of 0.4. The drag coefficient was taken to be 0.01. The maximum lift before stalling occurred on the blades was found to be less than for the straight bladed rotor described previously. The curves plotted for a blade rotation of −17 degrees are fictitious because stalling has occurred on the blades at this setting. The large angle of twist along the span of the blades meant that the outer blade elements stalled first while at lower angles of attack (i.e. lower blade rotations) the inner elements tended to be operating at large negative angles of incidence. This latter in particular is detrimental to the performance of the rotor. The three bladed rotor with a lower solidity operated at higher tip speed ratios.

Going back to considerations involving the first autogyro rotor (Autogyro A), with untwisted blades of constant chord, Figures 8, 9 and 10 have been plotted at blade rotations of 4, −2 and −8 degrees. Figure 8 shows the variation of the tip speed ratio with the angle of incidence. Figures 9 and 10 are plots of the total force coefficient C_{TA} and the aerodynamic drag angles ϵ_A. It can be seen that the variation of the drag angles with the angle of incidence tends to a straight line of unit slope as the blade rotation is adjusted towards the stall position (Figure 10). This is because the thrust forces from the rotor are much greater than

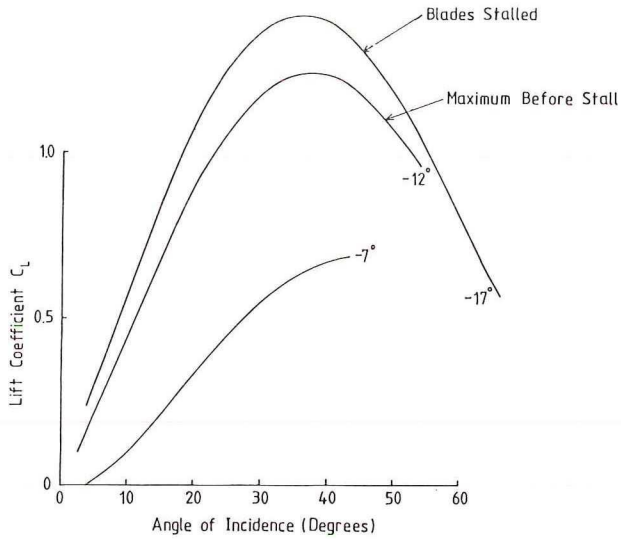

Figure 6. Lift coefficients of autogyro B. Numbers denote blade rotations.

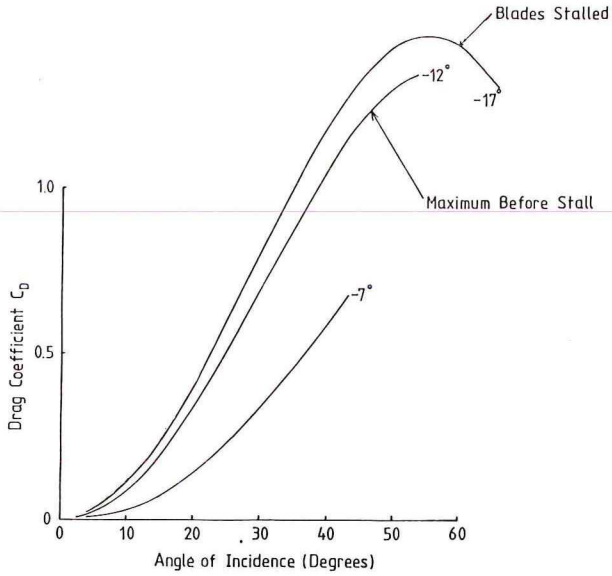

Figure 7. Drag coefficients of autogyro B. Numbers denote blade rotations.

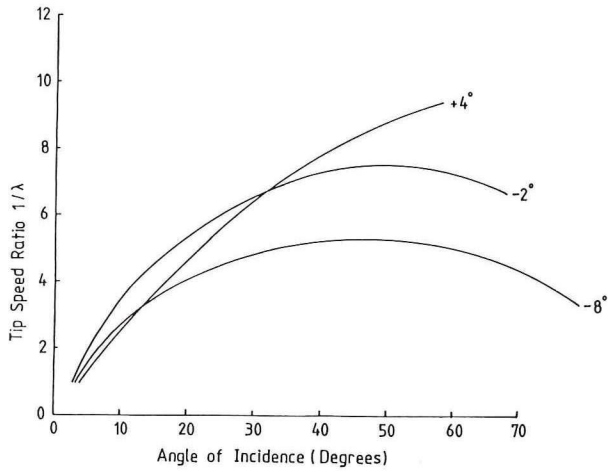

Figure 8. Variation of tip speed ratio with angle of incidence – autogyro A. Numbers denote blade rotations.

the downwind forces (H) over most of the useful range of operation. Since the largest force coefficients C_{TA} are produced just before stall occurs it follows that the best driving forces are obtained with the rotor at this blade setting. By comparing Figures 9 and 10 with Figure 11, which gives typical values of C_{TA} and ϵ_A plotted against β_A [16, 17] for a soft sail rig, it can be seen that the sail rig is superior over close hauled and close reaching cources (i.e. higher C_{TA} values at lower values of ϵ_A), but becomes inferior to this autogyro on reaching courses. On upwind courses the wind turbine would be used in the windmill mode.

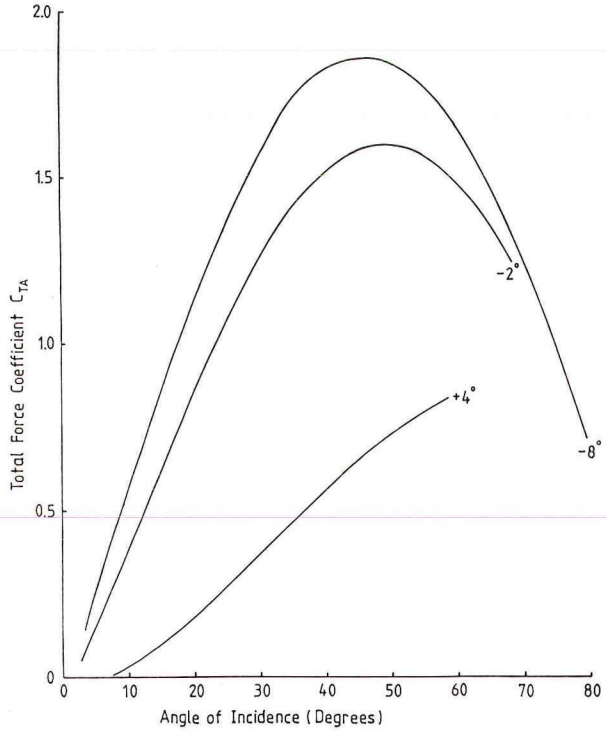

Figure 9. Total force coefficient – autogyro A. Numbers denote blade rotations.

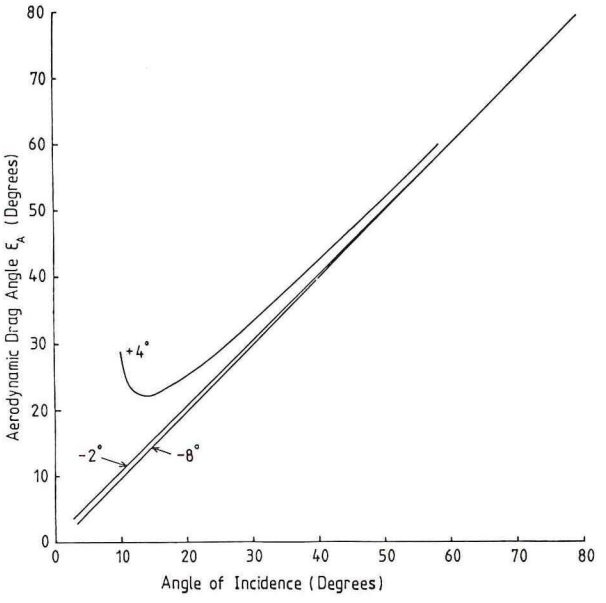

Figure 10. Aerodynamic drag angle – autogyro A. Numbers denote blade rotations.

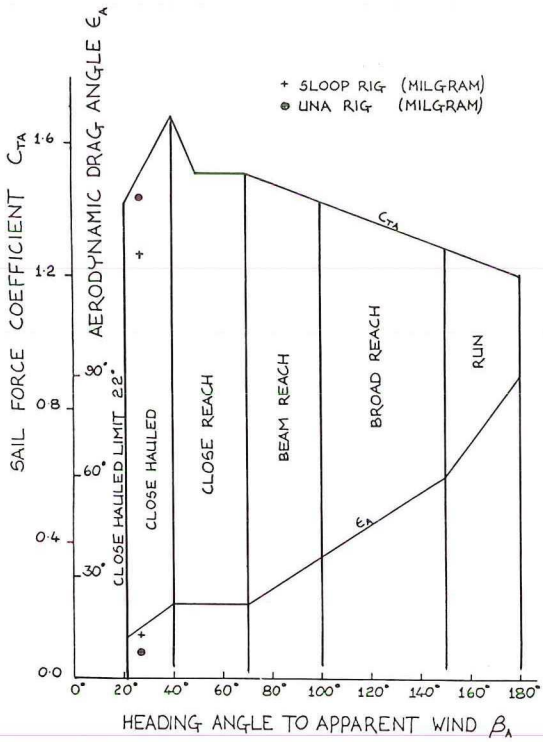

Figure 11. Estimated values of C_{TA} and β_A used in sail force calculations (Bradfield).

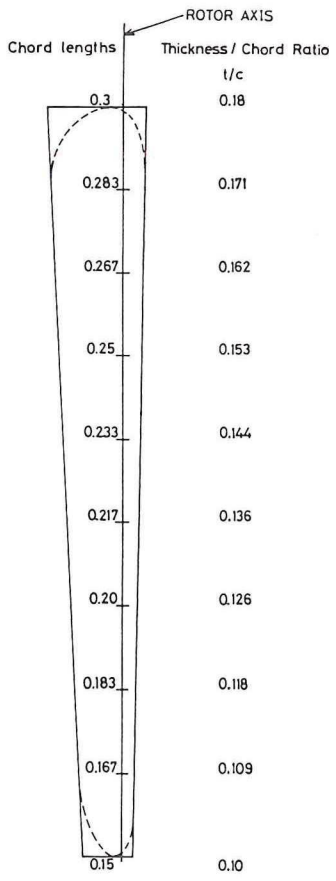

Figure 12. Geometry of rotor blade – autogyro B.

5. The autogyro as a propulsion system

The total force coefficient C_{TA} which has been calculated from the lift and drag coefficients of the rotor, is defined by

$$C_{TA} = \frac{T_A}{\frac{1}{2}\rho V^2 \pi R^2}$$

where T_A is the total force, ρ is the density of air and V is the apparent wind speed.

It is possible to resolve this force into a driving force F_R and a heeling force F_H, where

$$F_R = T_A \sin(\beta_A - \epsilon_A)$$
$$F_H = T_A \cos(\beta_A - \epsilon_A)$$

β_A is the apparent wind angle, the angle between the apparent wind V and the boat's course. These forces can also be written in their coefficient form as follows

$$C_R = C_{TA} \sin(\beta_A - \epsilon_A)$$
$$C_H = C_{TA} \cos(\beta_A - \epsilon_A)$$

The apparent wind angle and the apparent wind speed are given for any moving vehicle in the plane perpendicular to the mast as

$$\tan\beta_A = \frac{V_w}{V_b} \sin\alpha \cos\theta_h \Big/ \left(\frac{V_w}{V_b} \cos\alpha + 1\right)$$

$$V = V_b \sqrt{\left(\frac{V_w}{V_b} \sin\alpha \cos\theta_h\right)^2 + \left(\frac{V_w}{V_b} \cos\alpha + 1\right)^2}$$

where V_b is the speed of the boat, V_w is the true wind speed, α is the angle of the true wind to the boat's course and θ is the angle of heel.

To find the maximum driving force available from a given autogyro rotor it is necessary to maximise the value of C_R. C_{TA} and ϵ_A are known for the rotor for a range of angles of incidence, and it is found that the maximum value of C_R occurs at different angles of incidence depending on the value of β_A. Table 1, which shows the results for Glauert's example rotor, at a blade setting of $-2°$, illustrates this point. To obtain the best propulsive force during operation, the rotor will require to be trimmed to find this optimum angle.

6. Conclusion

The operation of a computer program which calculates the performance of a wind turbine when operating in the autogyro mode has been described. This program uses a method which has been extended for rotors with varying blade geometry from the methods developed for calculations on autogyros with fixed blades of constant section and chord. While ignoring the effects produced by the flapping motion of the blades which would be expected to reduce the performance of the autogyro by increasing the drag forces [5], although at the same time alleviating the adverse effects arising from the rolling moment, this approach was considered to be justified in allowing rapid calculations to be carried out for comparison purposes between different autogyro rotors. A comparison was made between two autogyro rotors which indicated in this case a better overall performance for the autogyro with straight, untwisted blades of constant chord. Twist along the blades of the rotor meant that the sections at different radii were not operating at their best positions on the lift curve slope at any one pitch setting. This indicates that variable pitch rotors which are designed for the propulsion of marine craft and are to be capable of operation in both the windmill and autogyro modes would have conflicting design requirements.

Acknowledgements

The author would like to thank the staff and technicians in the Department of Naval Architecture and Ocean Engineering at the University of Glasgow for

Table 1

Calculation of C_R for Glauert's example autogyro rotor at a blade setting of -2 degrees

angle of incidence α_i	tip speed ratio	C_{TA}	ϵ_A	$\beta_A = 45°$ C_R	$\beta_A = 60°$ C_R	$\beta_A = 90°$ C_R	$\beta_A = 120°$ C_R
4.8	1.99	0.14	5.4	0.09			
7.9	2.97	0.27	8.4	0.16			
11.7	3.92	0.46	12.1	0.25			
16.2	4.80	0.67	16.5	0.32	0.46		
21.2	5.60	0.90	21.4	0.36	0.56		
26.5	6.27	1.12	26.7	0.35	0.61		
31.8	6.80	1.31	32.0	0.29	0.62	1.11	1.31
37.1	7.18	1.46	37.3	0.19	0.56	1.16	1.45
42.2	7.41	1.55	42.3	0.07	0.47	1.14	1.51
46.9	7.52	1.60	47.0	−0.06	0.36	1.09	1.53
51.1	7.54	1.60	51.2	−0.17	0.24	1.00	1.49

their help with this work.

The work was undertaken with the support of a Marine Technology grant from the Science and Engineering Research Council.

Nomenclature

a	lift curve slope
B	number of blades
C_D	drag coefficient
C_H	heeling force coefficient
C_L	lift coefficient
C_R	driving force coefficient
C_{TA}	Total autogyro force coefficient
c	chord length
F_H	heeling force
F_R	driving force
H	longitudinal force
H_C	longitudinal force coefficient
H_1	longitudinal force on one blade
i	angle of incidence of the autogyro
L	rolling moment
L_C	rolling moment coefficient
L_1	rolling moment on one blade
Q	torque
Q_C	torque coefficient
Q_1	torque on one blade
R	radius of the autogyro
r	radius of blade element
T_A	total force
T	thrust force
T_C	thrust force coefficient
T_1	thrust force on one blade
U	inflow velocity at a blade element
U_x U_y	components of the inflow velocity U
u	axial velocity through the rotor disc
V	apparent wind velocity approaching the rotor
V_b	velocity of the ship/boat
V_w	true wind velocity
V'	resultant velocity experienced by the autogyro
v	axial induced velocity
x	coefficient of the axial velocity u as a function of ΩR
Y	side force
Y_C	side force coefficient
Y_1	side force on one blade
α	angle between the true wind direction and the ship's/boat's course
α_i	angle of incidence of the blade section
β	angular displacement of the blade
β_A	angle between the apparent wind direction and the ship's/boat's course
β_o	coning angle
δ	drag coefficient of the blade section
ϵ_A	aerodynamic drag angle
θ	blade element angle
θ_h	angle of heel
λ	speed ratio term $\lambda = V/\Omega R$
μ	coefficient of the velocity of side slip as a function of ΩR
ρ	density of air
ϕ	inflow angle
ψ	angle of rotation of the blade from the downwind position
Ω	rotational speed of the rotor

References

1. Rainey, R.C.T., 'The wind turbine ship', Symposium on Wind Propulsion of Commercial Ships, RINA, November 1980.
2. Wellicome, J., 'A broad appraisal of the economics and technical requisites for a wind driven merchant vessel', The Future of Commercial Sail, Occasional Publication No. 2, RINA 1975.
3. Hammitt, A.G., 'Technical Yacht Design', Adlard Coles, 1975.
4. Bose, N., 'Windmills – Propulsion for a hydrofoil trimaran', Symposium on Wind Propulsion of Commercial Ships, RINA, November 1980.
5. Glauert, H., and Durand, W.F. (Editor), 'Aerodynamic theory', Vol. IV, Julius Springer, 1935.
6. Klemin, A., 'The gyroplane sailboat', September 1935, Scientific American.
7. Moore-Brabazon, J.T.C., 'The autogyro rotor as a sail', 1934, Journal of the Royal Aeronautical Society, Vol. 38.
8. De La Cierva, J., 'The autogiro', 1930, Journal of the Royal Aeronautical Society.
9. De La Cierva, J., 'New developments of the autogiro', 1935, Journal of the Royal Aeronautical Society, Vol. 39.
10. Cleveland, R.M., 'Wings that turn', July 1935, Scientific American.
11. Bennett, J.A.J., 'The era of the autogyro', 1961, Journal of the Royal Aeronautical Society, Vol. 65, No. 610.
12. Caygill, L.E., and Nutt, A.E.W., 'Wind tunnel and dropping tests of autogyro models', November 1926, ARC R & M 1116.
13. Glauert, H., 'A general theory of the autogyro', ARC R & M 1111, November 1926.
14. Lock, C.N.H., 'Further development of autogyro theory', ARC R & M 1127, March 1927.
15. Wheatley, J.B., 'Aerodynamic analysis of the autogyro rotor with a comparison between calculated and experimental results', NACA Report 487, 1934.
16. Bradfield, W.S., 'Predicted and measured performance of a day-sailing catamaran', Marine Technology SNAME, January 1970.
17. Bose, N., 'Hydrofoils – Design of a wind propelled flying trimaran', PhD Thesis, University of Glasgow, April 1982.